Pairing of fermions under spin-orbit coupling in two dimensions

S. V. Andreev ●*

Physikalisches Institut, Albert-Ludwigs-Universität Freiburg, Hermann-Herder-Strasse 3, 79104 Freiburg, Germany

We present a theoretical approach to the problem of two-dimensional fermion pairing under spin-orbit (SO) coupling and Zeeman interaction with an external magnetic field. We introduce a generic pairing Hamiltonian operating in the Hilbert space spanning free pairs and bare two-body bound states. The SO coupling of Rashba or Dresselhaus type provides *p*-wave dressing of an *s*-wave spin-singlet bound state by continua in the triplet scattering channels. In the strong-coupling (Bose-Einstein condensate) limit of the many-body fermion system at zero temperature our theory maps onto the two-channel Fano-Anderson model of a spinless resonant *p*-wave superfluid.

I. INTRODUCTION

Pairing of fermions under spin-orbit (SO) coupling in two-dimensional (2D) crystals has been a central issue of the condensed matter physics over the past decades [1–11]. Rashba [12–14] or Dresselhaus [15,16] SO coupling in combination with transverse Zeeman splitting has been argued [3–6] to endow a conventional BCS superconductor with topological properties of the long-sought $p_x \pm i p_y$ Fermi superfluid [17,18]. The idea has readily been adopted to neutral ultracold atoms [4], where effective Zeeman splitting can be achieved by changing the population imbalance and the complications associated with the orbital motion of electrons in a transverse magnetic field do not arise. Atomic settings also enable the paradigmatic BCS-BEC crossover [19,20] by means of the Feshbach resonance [21]. However, experimental realization of the synthetic SO coupling [22,23] on top of the pairing remains challenging [24].

From the theoretical perspective, transparent analytical arguments have been provided for the BCS side of the crossover [6], the so-called weak-pairing regime [25]. The Bose-Einstein condensate (BEC) regime of tightly bound pairs (also referred to as strong-pairing limit) is far less understood. Recent numerical studies indicate that the precious topological aspect of the SO-coupled superfluidity survives in that regime for sufficiently large Zeeman splittings [11]. The critical magnetic field scales linearly with the pair binding energy [11].

In this paper, we present an insightful approach to the problem based on the second quantization in the basis of pair states. The theory inherits from our recent studies of SO-coupled pairing of electromagnetic bosons in 2D semiconductors [26]. We introduce a generic *pairing Hamiltonian* acting on free pairs and bare (i.e., without SO coupling) two-body bound states. For two particles in vacuum one obtains

a multichannel scattering theory, the channels being labeled by the projection of the pair spin on the transverse quantization axis (*z* axis) S_z. The SO coupling plays the role of a coherent switch between the channels. In particular, a bare *s*-wave bound state with $S_z = 0$ (spin singlet) transforms into a *p*-wave resonance due to the SO coupling to the continua of scattering states in the $S_z = \pm 1$ channels energetically detuned from the bound state by the magnetic field. One thus discovers a rich Feshbach resonancelike phenomenology. We predict giant *p*-wave halos carrying synthetic angular momenta $L_z = \pm \hbar$. For a Fermi superfluid in the strong-coupling regime, our theory maps onto the two-channel Fano-Anderson model [27,28] of a spinless resonant *p*-wave superfluid. This model has been extensively studied in the context of resonant Fermi superfluids of ultracold atoms [31]. The coherent Feshbach link between "open" and "closed" scattering channels in a typical atomic setting is due to the hyperfine interaction [21]. The SO coupling may then be added on top of it as an independent ingredient [24]. In our case, the SO coupling itself plays the role of the Feshbach-type link. Such a link, however, has a nontrivial dynamical (orbital) nature, that provides *p*-wave dressing of the bare *s*-wave bound state. The topological properties of the Bogoliubov transformation, existence of Majorana fermions in the vortex cores, and helical edge states [17] then follow automatically. At fixed binding energy of the bare molecule the topological transition is realized by the Zeeman tuning of the lower-energy triplet channel across the resonance. One thus recovers the linear scaling of the critical magnetic field with the binding energy reported in the earlier work [11]. The quantum halos may be regarded as precursors of the *p*-wave Cooper pairs enabling the topological superfluidity on the BCS side of the transition. In contrast to the Cooper pairs, the halos may equally well exist in vacuum and are expected to be more robust to thermal fluctuations.

The paper is organized as follows. We first provide a more detailed statement of the problem and discuss its scope (Sec. II). In Sec. III we provide some guiding arguments for our discussion by using the familiar language. In Sec. IV,

*Serguey.Andreev@gmail.com

we present our approach. We introduce a generic second-quantized pair Hamiltonian and discuss its properties. In particular, we point out destructive interference of the Feshbach links associated with SO-induced spin flips due to the center-of-mass motion of two fermions. This makes possible the standard identification of a dressed four-leg vertex function with the two-body scattering T matrix in vacuum. The corresponding discussion opens Sec. V. After having discussed the two-body scattering (Sec. V A) and emergence of the p-wave halo (Sec. V B), we unveil the intrigue of the topological phase transition in the BEC limit (Sec. V C). We close that section by a brief demonstration of direct correspondence of our theory to the familiar arguments in the limiting case of weak pairing. Finally, we discuss experimental detection of the halos and speculate on possible implementation of the topological superconductivity in cuprates.

II. STATEMENT OF THE PROBLEM

We consider a binary mixture of spin-up $|\uparrow\rangle$ and spin-down $|\downarrow\rangle$ fermions constrained to move in two dimensions (2D). The (grand canonical) Hamiltonian reads as

$$\hat{H} = \sum_{\boldsymbol{p},\sigma,\sigma'=\uparrow,\downarrow} [\xi_{\boldsymbol{p}} \delta_{\sigma\sigma'} - \hbar\boldsymbol{\omega}(\boldsymbol{p}) \cdot \boldsymbol{s}_{\sigma\sigma'}] \hat{a}^{\dagger}_{\sigma,\boldsymbol{p}} \hat{a}_{\sigma',\boldsymbol{p}}$$
$$+ \frac{1}{2S} \sum_{\boldsymbol{p}_1,\boldsymbol{p}_2,\boldsymbol{q},\sigma,\sigma'} \hat{a}^{\dagger}_{\sigma,\boldsymbol{p}_1+\boldsymbol{q}} \hat{a}^{\dagger}_{\sigma',\boldsymbol{p}_2-\boldsymbol{q}} V_{\sigma\sigma'}(\boldsymbol{q}) \hat{a}_{\sigma',\boldsymbol{p}_2} \hat{a}_{\sigma,\boldsymbol{p}_1}, \quad (1)$$

where, according to the common notation,

$$\xi_{\boldsymbol{p}} \equiv \frac{\hbar^2 p^2}{2m} - \mu \quad (2)$$

and $V_{\sigma\sigma'}(\boldsymbol{q}) = \int e^{-i\boldsymbol{q}\boldsymbol{r}} V_{\sigma\sigma'}(\boldsymbol{r}) d\boldsymbol{r}$ are the Fourier transforms of the two-body interaction potentials. The annihilation operators $\hat{a}_{\sigma,\boldsymbol{p}}$ for fermions are labeled by z projection σ of their spin

$$\boldsymbol{s} = \frac{1}{2}(\hat{\sigma}_x \boldsymbol{n}_x + \hat{\sigma}_y \boldsymbol{n}_y + \hat{\sigma}_z \boldsymbol{n}_z) \quad (3)$$

and the momentum $\boldsymbol{p} = (p_x, p_y)$ of their in-plane translational motion. Here the vectors $\boldsymbol{n}_x$, $\boldsymbol{n}_y$, and $\boldsymbol{n}_z$ form an orthonormal basis in the real space. The operators $\hat{a}_{\sigma,\boldsymbol{p}}$ obey the commutation relations

$$\{\hat{a}_{\sigma,\boldsymbol{p}}, \hat{a}^{\dagger}_{\sigma',\boldsymbol{p}'}\} = \delta_{\sigma\sigma'} \delta_{\boldsymbol{p}\boldsymbol{p}'},$$
$$\{\hat{a}_{\sigma,\boldsymbol{p}}, \hat{a}_{\sigma',\boldsymbol{p}'}\} = 0. \quad (4)$$

The mixture is characterized by the unique chemical potential μ and the population imbalance is due to Zeeman splitting of the spin sublevels in a generalized magnetic field characterized by the Larmour frequency

$$\boldsymbol{\omega}(\boldsymbol{p}) = \boldsymbol{\Omega}(\boldsymbol{p}) + \frac{\mu_B}{\hbar} g B \boldsymbol{n}_z, \quad (5)$$

that includes the effect of SO coupling in the form of an effective momentum-dependent magnetic field. Equivalently, one could model the Zeeman splitting due to the transverse magnetic field $\boldsymbol{B} = B\boldsymbol{n}_z$ by introducing two chemical potentials $\mu_{\pm} = \mu \pm \mu_B g B/2$. For definitiveness, hereinafter we shall adopt the former way.

The vector $\boldsymbol{\Omega}(\boldsymbol{p})$ is assumed to lie in the xy plane. Invariance of the fermionic Hamiltonian (1) with respect to the time
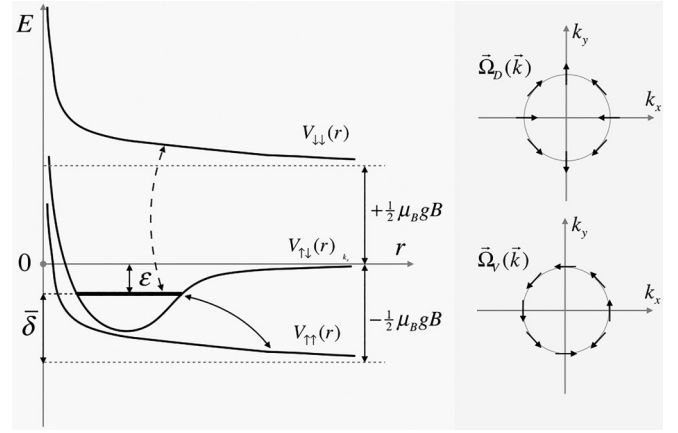

FIG. 1. Schematic illustration of the interaction potentials (on the left) and effective SO fields (on the right). The scattering channels are split by an external magnetic field. The curved arrows (solid and dashed) depict possible coherent couplings between the bound state and the continua of scattering states performed by the SO fields. The solid curved arrow corresponds to the resonant approximation employed in Sec. V.

reversal requires

$$\boldsymbol{\Omega}(-\boldsymbol{p}) = -\boldsymbol{\Omega}(\boldsymbol{p}). \quad (6)$$

Explicitly, in most cases of interest one deals with the following two types of SO coupling:

$$\boldsymbol{\Omega}_D(\boldsymbol{p}) = -\upsilon_D p(\boldsymbol{n}_x \cos\theta - \boldsymbol{n}_y \sin\theta), \quad (7)$$

the so-called Dresselhaus SO coupling [15] written in the 2D form (7) by Dyakonov and Kachorovskii [16] and

$$\boldsymbol{\Omega}_R(\boldsymbol{p}) = -\upsilon_R p(\boldsymbol{n}_x \sin\theta - \boldsymbol{n}_y \cos\theta), \quad (8)$$

known as Rashba SO coupling [12]. The 2D form (8) was derived by Vas'ko [13] and exploited by Bychkov and Rashba a few years later [14]. Here p and θ are the polar coordinates of $\boldsymbol{p}$, and the material-specific parameters $\upsilon_{D,R}$ have the dimension of the velocity. We shall focus on the Rashba SO coupling (8) in order to be in line with the previous studies [1,4–6,9,11].

We now discuss in more detail the interaction part of the Hamiltonian (1). We shall make use of the renown toy model of the BEC-BCS crossover [19,29], where discussion of the actual pairing mechanism is left aside and the pairing instability is due to a bound state in a hypothetical static potential $V_{\uparrow\downarrow}(\boldsymbol{r})$ schematically illustrated in Fig. 1. Strong arguments in favor of the ensuing phenomenology have recently been provided for high-temperature superconducting cuprates [30]. For our purposes and for the sake of transparency, it is sufficient to assume that there is a unique s-wave bound state. This bound state may additionally be separated from the corresponding (spin-singlet) continuum by a repulsive potential barrier. In this case the bound state can transform into a 2D resonance upon shallowing the potential well. Such upgrade allows one to account for a possible resonant pairing scenario, pertinent to ultracold atoms [21,31]. Introduction of the SO coupling in this case may yield a peculiar *folded* resonance, implicitly encountered in our earlier work on bosons [26].

Detailed discussion of this possibility goes beyond the scope of this study and we shall postpone it to future work. Bearing in mind the Pauli exclusion principle, we assume the background potentials $V_{\uparrow\uparrow}(\mathbf{r})$ and $V_{\downarrow\downarrow}(\mathbf{r})$ to be featureless (no bound states or resonances). In Fig. 1 these are tentatively sketched as short-range repulsive potentials. All potentials are assumed to be axially symmetric: the interaction term alone conserves angular momenta of the pairs.

We shall refer to the zero-temperature many-body phase diagram of the model (1) with $\boldsymbol{\omega}(\mathbf{p}) \equiv 0$ as *bare* BCS-BEC crossover. It is realized by varying either the chemical potential μ or the energy of the discrete level ε. For the pairing potential of the type shown in Fig. 1 a thermodynamically smooth crossover occurs in the vicinity of the characteristic point $\mu = 0$ [29]. For the resonant shape (not shown) there would be a well-defined crossover region, where the BCS superfluid coexists with a molecular BEC: the crossover starts at $2\mu = \varepsilon$ and terminates at $\mu = 0$ [31]. At that lower bound almost all Cooper pairs are converted into the molecules. A qualitative connection between the two scenarios is established by letting the resonance width Γ go to infinity (i.e., by suppressing the repulsive potential barrier).

III. PRELIMINARIES

Let us consider the BCS side of the (bare) crossover in the presence of SO coupling and magnetic field. We replace the s-wave pairing potential $V_{\uparrow\downarrow}(\mathbf{k}' - \mathbf{k})$ in the Hamiltonian (1) by an attractive separable force

$$V_{\uparrow\downarrow}(\mathbf{k}', \mathbf{k}) \equiv \epsilon \chi^*(k')\chi(k)S, \tag{9}$$

where the quantization area S on the right-hand side has been singled out for further convenience, so that the parameter

$\epsilon < 0$ characterizing the strength of the attraction has the units of energy. The relative momentum $\mathbf{k}$ enters the dimensionless monotonously decaying function $\chi(k)$ as a product ka, with a characterizing the spatial extent of the force. For simplicity, we switch off the background repulsive interactions by setting $V_{\uparrow\uparrow}(\mathbf{r}) = V_{\downarrow\downarrow}(\mathbf{r}) \equiv 0$. Following the standard prescription, we introduce the anomalous average

$$\Delta = \epsilon \sum_{\mathbf{k}} \chi(k)\langle \hat{a}_{\downarrow,-\mathbf{k}}\hat{a}_{\uparrow,\mathbf{k}}\rangle \tag{10}$$

over the bare BCS ground state. The arbitrary complex phases of both $\chi(k)$ and Δ can be set identically zero, but hereinafter we shall keep the sign of the complex conjugate for the aesthetic reasons.

We diagonalize the single-particle part of (1) by the substitution

$$\hat{a}_{\uparrow,\mathbf{p}} = \frac{1}{\mathcal{N}}\left(\frac{\hbar\boldsymbol{\Omega}(\mathbf{p})\cdot \mathbf{s}_{\uparrow\downarrow}}{\frac{1}{2}\hbar\omega(\mathbf{p}) + \frac{1}{2}\mu_B g B}\hat{b}_{+,\mathbf{p}} - \hat{b}_{-,\mathbf{p}}\right),$$

$$\hat{a}_{\downarrow,\mathbf{p}} = \frac{1}{\mathcal{N}}\left(\hat{b}_{+,\mathbf{p}} + \frac{\hbar\boldsymbol{\Omega}(\mathbf{p})\cdot \mathbf{s}_{\downarrow\uparrow}}{\frac{1}{2}\hbar\omega(\mathbf{p}) + \frac{1}{2}\mu_B g B}\hat{b}_{-,\mathbf{p}}\right),$$

with

$$\mathcal{N} = \sqrt{\frac{2\hbar\omega(\mathbf{p})}{\hbar\omega(\mathbf{p}) + \mu_B g B}}.$$

We have defined the matrix element $\mathbf{s}_{\uparrow\downarrow} \equiv \langle\uparrow|\hat{\mathbf{s}}|\downarrow\rangle$. Assuming $\mu < \mu_B g B/2$ and

$$\Delta \ll \mu_B g B - 2\mu \tag{11}$$

we adiabatically eliminate the upper band and obtain the projected Hamiltonian

$$\hat{H}^{(--)} = \sum_{\mathbf{p}} \zeta_{-,\mathbf{p}}\hat{b}^{\dagger}_{-,\mathbf{p}}\hat{b}_{-,\mathbf{p}} + \epsilon\sum_{\mathbf{k}',\mathbf{k}}\chi^*(k')\frac{\boldsymbol{\Omega}^{(a)}(\mathbf{k}')\cdot \mathbf{s}_{\uparrow\downarrow}}{\omega(k')}\hat{b}^{\dagger}_{-,\mathbf{k}'}\hat{b}^{\dagger}_{-,-\mathbf{k}'}\chi(k)\frac{\boldsymbol{\Omega}^{(a)}(\mathbf{k})\cdot \mathbf{s}_{\downarrow\uparrow}}{\omega(k)}\hat{b}_{-,-\mathbf{k}}\hat{b}_{-,\mathbf{k}}$$

$$- \epsilon\sum_{\mathbf{k}',\mathbf{k}}\chi^*(k')\frac{\boldsymbol{\Omega}^{(a)}(\mathbf{k}')\cdot \mathbf{s}_{\uparrow\downarrow}}{\omega(k')}\hat{b}^{\dagger}_{-,\mathbf{k}'}\hat{b}^{\dagger}_{-,-\mathbf{k}'}\chi(k)\frac{\mu_B g B}{\hbar\omega(k)}\hat{b}_{+,-\mathbf{k}}\hat{b}_{-,\mathbf{k}} - \text{H.c.}, \tag{12}$$

where

$$\zeta_{\pm,\mathbf{p}} = \xi_{\mathbf{p}} \pm \frac{1}{2}\hbar\omega(p) \tag{13}$$

and we have taken advantage of the anticommutation relations (4) and the symmetry of $\boldsymbol{\Omega}(\mathbf{k})$ with respect to the time reversal (6) to define

$$\boldsymbol{\Omega}^{(a)}(\mathbf{k}) \equiv \frac{\boldsymbol{\Omega}(\mathbf{k}) - \boldsymbol{\Omega}(-\mathbf{k})}{2}. \tag{14}$$

Note, that the last term in Eq. (12) should be retained under the condition (11).

Let us start with the Zeeman splitting only and gradually increase the SO coupling strength. In the first order, we write

$$\hat{b}_{-,-\mathbf{k}}\hat{b}_{-,\mathbf{k}} = \hat{a}_{\uparrow,-\mathbf{k}}\hat{a}_{\uparrow,\mathbf{k}} + \frac{\hbar\boldsymbol{\Omega}^{(a)}(\mathbf{k})\cdot \mathbf{s}_{\uparrow\downarrow}}{\frac{1}{2}\mu_B g B}\langle\hat{a}_{\downarrow,-\mathbf{k}}\hat{a}_{\uparrow,\mathbf{k}}\rangle, \tag{15a}$$

$$\hat{b}_{+,-\mathbf{k}}\hat{b}_{-,\mathbf{k}} = -\langle\hat{a}_{\downarrow,-\mathbf{k}}\hat{a}_{\uparrow,\mathbf{k}}\rangle + \frac{\boldsymbol{\Omega}^{(a)}(\mathbf{k})\cdot \mathbf{s}_{\downarrow\uparrow}}{\mu_B g B}\hat{a}_{\uparrow,-\mathbf{k}}\hat{a}_{\uparrow,\mathbf{k}}. \tag{15b}$$

Before we proceed, it is instructive to consider the two-body scattering in vacuum by putting $\mu \to -\mu_B g B/2$. In this limit one may omit the last term (and its H.c.) in the projected Hamiltonian (12) [under the assumption (11) this term comes into play only when μ approaches 0] and discover that the SO coupling results in *an effective p-wave attraction* between the spin-$\uparrow$ fermions

$$V_{\uparrow\uparrow}^{(\text{eff})}(\mathbf{k}', \mathbf{k}) \equiv \epsilon\hbar^2 v_R^2 \frac{\chi^*(k')\chi(k)k'k}{(\mu_B g B)^2}e^{i(\theta'-\theta)}S, \tag{16}$$

where we have borne in mind the Rashba expression (8) for the SO field $\boldsymbol{\Omega}(\mathbf{k})$. This attraction is certainly too weak to produce a polarized bound state (the total spin $S_z = +1$). The

latter would require an energy scale of $V_{\uparrow\downarrow}(\mathbf{k}', \mathbf{k})$ comparable to the Zeeman splitting $\mu_B g B$. But, this circumstance does not exclude a p-wave pairing instability, even despite that we are in 2D [25,29]. Indeed, below we show that unconventional p-wave pairing of the polarized spin-$\uparrow$ Fermi sea takes place in this model.

By substituting Eqs. (15) into (12), using the Wick's theorem and omitting full averages, we replace the Hamiltonian (12) by the BCS form [6]

$$\hat{H}_{\text{BCS}}^{(--)} = \sum_{\mathbf{p}} \zeta_{-,\mathbf{p}} \hat{a}_{\uparrow,\mathbf{p}}^{\dagger} \hat{a}_{\uparrow,\mathbf{p}} + \sum_{\mathbf{k}} (\Delta_{--}^{*} \hat{a}_{\uparrow,-\mathbf{k}} \hat{a}_{\uparrow,\mathbf{k}} + \text{H.c.}),$$
(17)

where we have defined

$$\Delta_{--} \equiv \frac{\hbar \mathbf{\Omega}^{(a)}(\mathbf{p}) \cdot \mathbf{s}_{\uparrow\downarrow}}{\mu_B g B} \Delta = i \frac{\Delta}{2\mu_B g B} \hbar v_R p e^{-i\theta}$$
(18)

and absorbed the Hartree-Fock shift of the quasiparticle energy into the chemical potential μ. The projected BCS Hamiltonian (17) is characterized by broken time-reversal symmetry and nontrivial topology of the Bogoliubov coefficients $u_{\uparrow,\mathbf{k}}$ and $v_{\uparrow,\mathbf{k}}$ that define the long-distance behavior of the (in-medium) pair wave function

$$g_{\uparrow\uparrow}(\mathbf{r}) = \frac{1}{S} \sum_{\mathbf{k}} g_{\uparrow\uparrow,\mathbf{k}} e^{i\mathbf{k}\mathbf{r}}$$
(19)

via its Fourier transform

$$g_{\uparrow\uparrow,\mathbf{k}} = \frac{v_{\uparrow,\mathbf{k}}}{u_{\uparrow,\mathbf{k}}} = -\frac{\sqrt{\zeta_{-,\mathbf{k}}^2 + |\Delta_{--}|^2} - \zeta_{-,\mathbf{k}}}{\Delta_{--}^{*}}.$$
(20)

Namely, as $\mathbf{k} \to 0$, one has $g_{\uparrow\uparrow,\mathbf{k}} \propto 1/(k_x - ik_y)$ and $g_{\uparrow\uparrow}(\mathbf{r}) \propto 1/z$ with $z = x - iy$, which is characteristic for the Moore-Read (Pfaffian) state in the fractional quantum Hall effect [17].

As μ approaches the upper band and the condition (11) gets violated, a topological phase transition occurs into the conventional BCS superfluid due to onset of the inter-band s-wave pairing in the full (nonprojected) model

$$\hat{H}_{\text{BCS}} = \sum_{\mathbf{p},\alpha=+,-} \zeta_{\alpha,\mathbf{p}} \hat{b}_{\alpha,\mathbf{p}}^{\dagger} \hat{b}_{\alpha,\mathbf{p}}$$

$$+ \sum_{\mathbf{k}} (\Delta_{++} \hat{b}_{+,-\mathbf{k}} \hat{b}_{+,\mathbf{k}} + \Delta_{--} \hat{b}_{-,-\mathbf{k}} \hat{b}_{-,\mathbf{k}}$$

$$+ \Delta_{+-} \hat{b}_{+,-\mathbf{k}} \hat{b}_{-,\mathbf{k}} + \text{H.c.}),$$
(21)

with $\Delta_{++} = \Delta_{--}^{*}$ and

$$\Delta_{+-} = \frac{\mu_B g B}{\hbar \omega(\mathbf{p})} \Delta.$$
(22)

Note also the restoration of the time-reversal symmetry as the upper band comes into play. A fully analytical description of this transition is not available because of the necessity to keep all contributions from both bands, which is a nontrivial task. Nevertheless, the underlying phenomenology is rather well understood [5,7]. At $B \to 0$ the interband pairing is again suppressed, but there is no topological transition since now the anomalous averages build up simultaneously within both bands of opposite chirality [1].

The model (17) has primarily been known [17] to exhibit a topological phase transition from the weak to strong pairing regime, where the function $\zeta_{-,0}$ becomes negative. This transition is not accessible within our current approximation, for, to push the chemical potential μ below the bottom of the band, one would need a true $S_z = +1$ bound state and, as we have just seen, the latter is impossible in the frame of the Hamiltonian (12). One could expect that such kind of transition becomes available on the strong-pairing (BEC) side of the bare crossover. In contrast to the aforementioned transition to the conventional state within the weak-pairing scheme, the new transition should occur at high magnetic fields, where the time reversal is effectively broken. However, the condition (11) is no longer fulfilled, so that one cannot employ the drastic simplifications made above to achieve the canonical p-wave BCS form (17). Not to say that the very BCS approach remains valid only qualitatively on the BEC side. The problem represents an apparent challenge for the theory.

IV. PAIRING FORMALISM

A. Motivation

Consider a system of two fermions in vacuum. There are four basis states $|\uparrow\uparrow\rangle$, $|\uparrow\downarrow\rangle$, $|\downarrow\uparrow\rangle$, $|\downarrow\downarrow\rangle$ whose linear combinations realize the states $S_z = +1, 0, -1$ of the total spin $S_z = s_{z,1} + s_{z,2}$. We notice that since the effective magnetic field $\mathbf{\Omega}(\hat{\mathbf{p}}_i)$ lies in the structure plane, the sum $\mathbf{\Omega}(\hat{\mathbf{p}}_1) \cdot \hat{\mathbf{s}}_1 + \mathbf{\Omega}(\hat{\mathbf{p}}_2) \cdot \hat{\mathbf{s}}_2$ does not commute with S_z^2. Hence, the SO coupling may change the spin state of a pair by flipping the spin of either of the two particles.

We have just seen in Sec. III that in a strong magnetic field such spin flips are at the origin of the pairing instability in a nominally normal polarized Fermi sea. In the two-fermion language the surface of the sea may be regarded as an *open channel* for the (quasi)particle scattering. Equations (12), (15), and (17) suggest that the p-wave attraction in the open channel can be seen as due to the SO coupling to the *closed molecular channel*: the magnetic-field detuned s-wave bound state of the pairing potential $V_{\uparrow\downarrow}(r)$. On the BCS side of the bare crossover, the closed channel is energetically well above the scattering threshold in the open channel. On the BEC side, in contrast, the strongly bound state may come into *resonance* with the polarized Fermi sea. The two-fermion picture adopted in this section seems to be particularly convenient for description of such situation.

In principle, the above hints alone are sufficient to construct the corresponding two-body scattering theory in vacuum. A more advanced formalism based on the second quantization that we develop below aims at solution of the full many-body problem. As an important first step, one may follow the standard Bogoliubov prescription consisting in replacement of second-quantized operators by c-numbers. We shall see that in the strong-pairing limit our theory maps onto the two-channel Fano-Anderson model [27,28] of a spinless resonant p-wave superfluid, thoroughly investigated in the context of ultracold atoms [31]. Many interesting conclusions then follow immediately. Our pairing formalism may also serve as a basis and, simultaneously, a valuable

guidance for the development of a diagrammatic theory and study of the beyond-mean-field effects. The proper two-body scattering theory will follow automatically as a limiting case.

B. Pairing Hamiltonian

We start with the single-particle Hamiltonian used to construct the second-quantized equation (1):

$$\hat{H}_i = \hat{K}_i + \hat{H}_{\boldsymbol{\omega},i}, \tag{23}$$

where

$$\hat{K}_i = -\frac{\hbar^2 \nabla_i^2}{2m} \hat{1}_i \tag{24}$$

with

$$\hat{1}_i = \begin{bmatrix} 1 & 0 \\ 0 & 1 \end{bmatrix}_i \tag{25}$$

being the unity matrix and

$$\hat{H}_{\boldsymbol{\omega},i} = \begin{bmatrix} -\frac{1}{2}\mu_B gB & \hbar\boldsymbol{\Omega}(\hat{\boldsymbol{p}}_i) \cdot \boldsymbol{s}_{\uparrow\downarrow} \\ \hbar\boldsymbol{\Omega}(\hat{\boldsymbol{p}}_i) \cdot \boldsymbol{s}_{\downarrow\uparrow} & \frac{1}{2}\mu_B gB \end{bmatrix}_i, \tag{26}$$

where the index i labels the particle and we have used the spin-up $|\uparrow\rangle$ and spin-down $|\downarrow\rangle$ basis introduced previously. We build the 4×4 matrix by performing the so-called Kronecker summation of the single-particle 2×2 Hamiltonians (23) for two particles

$$\hat{\mathcal{H}} = \hat{H}_1 \oplus \hat{H}_2 \equiv \hat{H}_1 \otimes \hat{1}_2 + \hat{1}_1 \otimes \hat{H}_2. \tag{27}$$

This composite matrix will play the same role in our pair second-quantization procedure as the Hamiltonian (23) in the conventional second quantization. The pair Hamiltonian admits the useful decomposition

$$\hat{\mathcal{H}} = \hat{\mathcal{H}}_{\text{c.m.}} + \hat{\mathcal{H}}_{\text{rel}}, \tag{28}$$

where $\hat{\mathcal{H}}_{\text{c.m.}}$ acts on the center-of-mass (c..m.) coordinate of the two particles

$$\boldsymbol{R} = \frac{\boldsymbol{r}_1 + \boldsymbol{r}_2}{2} \tag{29}$$

and $\hat{\mathcal{H}}_{\text{rel}}$ acts on the coordinate of the relative motion

$$\boldsymbol{r} = \boldsymbol{r}_1 - \boldsymbol{r}_2. \tag{30}$$

The two-body interaction in the new basis is represented by a diagonal matrix

$$\hat{\mathcal{V}} = \sum_{\sigma,\sigma'} V_{\sigma\sigma'}(r) |\sigma\sigma'\rangle \langle\sigma\sigma'|. \tag{31}$$

The bound states of the potential $V_{\uparrow\downarrow}(\boldsymbol{r})$ are the solutions of the one-channel Schrödinger equation

$$\langle\uparrow\downarrow| (\hat{\mathcal{H}}_{\text{rel}} + \hat{\mathcal{V}}) |\uparrow\downarrow\rangle \varphi_n(\boldsymbol{r}) = \varepsilon_n \varphi_n(\boldsymbol{r}), \tag{32}$$

where the index n stands for a full set of possible quantum numbers.

We now have all ingredients to proceed with the second quantization. We introduce the (free) pair creation and annihilation operators

$$\begin{aligned} \hat{C}^\dagger_{\sigma_1\sigma_2,\boldsymbol{k},\boldsymbol{K}} &= \hat{a}^\dagger_{\sigma_1\boldsymbol{k}+\boldsymbol{K}/2} \hat{a}^\dagger_{\sigma_2,-\boldsymbol{k}+\boldsymbol{K}/2}, \\ \hat{C}_{\sigma_1\sigma_2,\boldsymbol{k},\boldsymbol{K}} &= \hat{a}_{\sigma_2,-\boldsymbol{k}+\boldsymbol{K}/2} \hat{a}_{\sigma_1\boldsymbol{k}+\boldsymbol{K}/2}, \end{aligned} \tag{33}$$

where $\boldsymbol{k} = (\boldsymbol{p}_1 - \boldsymbol{p}_2)/2$ and $\boldsymbol{K} = \boldsymbol{p}_1 + \boldsymbol{p}_2$ are the relative and c..m. momenta, respectively. By virtue of the anticommutation relations (4) one has

$$\hat{C}_{\sigma_1\sigma_2,\boldsymbol{k},\boldsymbol{K}} = -\hat{C}_{\sigma_2\sigma_1,-\boldsymbol{k},\boldsymbol{K}}. \tag{34}$$

Next, we define the molecular operators

$$\hat{C}_{\uparrow\downarrow,n,\boldsymbol{K}} = \sum_{\boldsymbol{k}} \phi_n(\boldsymbol{k}) \hat{C}_{\uparrow\downarrow,\boldsymbol{k},\boldsymbol{K}}, \tag{35}$$

where the function $\phi_n(\boldsymbol{k})$ is the Fourier image of the molecular wave function of the relative motion

$$\varphi_n(\boldsymbol{r}) = \frac{1}{\sqrt{S}} \sum_{\boldsymbol{k}} \phi_n(\boldsymbol{k}) e^{i\boldsymbol{k}\boldsymbol{r}}, \tag{36}$$

with S being the quantization area.

In terms of the free-pair and molecular operators the second-quantized *pairing Hamiltonian* can be written as

$$\hat{H} = \frac{1}{2} \sum_{\sigma'_1\sigma'_2\sigma_1\sigma_2} \sum_{\boldsymbol{k}',n',\boldsymbol{k},n} \sum_{\boldsymbol{K}',\boldsymbol{K}} \mathcal{H}^{\boldsymbol{k}'(n'),\boldsymbol{K}',\boldsymbol{k}(n),\boldsymbol{K}}_{\sigma'_1\sigma'_2\sigma_1\sigma_2} \hat{C}^\dagger_{\sigma'_1\sigma'_2,\boldsymbol{k}'(n'),\boldsymbol{K}'} \hat{C}_{\sigma_1\sigma_2,\boldsymbol{k}(n),\boldsymbol{K}}, \tag{37}$$

where we have used the obvious notation $\hat{C}_{\sigma_1\sigma_2,n,\boldsymbol{K}} \equiv \delta_{\sigma_1\bar{\sigma}_2} \hat{C}_{\uparrow\downarrow,n,\boldsymbol{K}}$ with $\bar{\sigma}$ meaning the reverse of σ, i.e., for $\sigma =\uparrow$ one has $\bar{\sigma} =\downarrow$ and vice versa. From a mathematical viewpoint, the form (37) is dictated by the principle of asymptotic completeness of the ensuing scattering theory [32]. The matrix elements

$$\mathcal{H}^{\boldsymbol{k}'(n'),\boldsymbol{K}',\boldsymbol{k}(n),\boldsymbol{K}}_{\sigma'_1\sigma'_2\sigma_1\sigma_2} = \int \psi^*_{\boldsymbol{k}'(n'),\boldsymbol{K}'}(\boldsymbol{r},\boldsymbol{R}) \langle\sigma'_1\sigma'_2| \hat{\mathcal{H}} |\sigma_1\sigma_2\rangle \psi_{\boldsymbol{k}(n),\boldsymbol{K}}(\boldsymbol{r},\boldsymbol{R}) d\boldsymbol{r}\, d\boldsymbol{R} \tag{38}$$

are taken on the free and bound state wave functions

$$\psi_{\boldsymbol{k}\boldsymbol{K}}(\boldsymbol{r},\boldsymbol{R}) = \frac{1}{S} e^{i\boldsymbol{k}\boldsymbol{r}+i\boldsymbol{K}\boldsymbol{R}}, \tag{39a}$$

$$\psi_{n,\boldsymbol{K}}(\boldsymbol{r},\boldsymbol{R}) = \frac{1}{\sqrt{S}} e^{i\boldsymbol{K}\boldsymbol{R}} \varphi_n(\boldsymbol{r}). \tag{39b}$$

C. Discussion

Let us analyze Eq. (37) in more detail. For simplicity, we let $B = 0$ (no Zeeman splitting). Consider first diagonal contributions to Eq. (37). These consist of the terms due to the scattering states and the terms due to the bound state. The diagonal contribution due to the scattering states
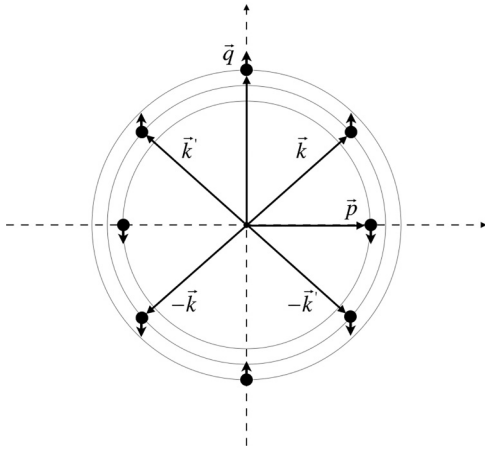
FIG. 2. Particle occupation configuration used to demonstrate the duality between the diagonal part of the pairing Hamiltonian and the conventional construction in terms of the particle operators $\hat{a}_{\sigma,k}$.

reads as

$$\frac{1}{2}\sum_{\sigma_1,\sigma_2}\sum_{k,K}[K_{\mathrm{c.m.}}(K) + K_{\mathrm{rel}}(k)]\hat{C}^\dagger_{\sigma_1\sigma_2,k,K}C_{\sigma_1\sigma_2,k,K}$$
$$+\frac{1}{2S}\sum_{\sigma_1,\sigma_2}\sum_{k,k',K}V_{\sigma_1\sigma_2}(k'-k)\hat{C}^\dagger_{\sigma_1\sigma_2,k',K}C_{\sigma_1\sigma_2,k,K}, \quad (40)$$

where we have used the obvious notations $K_{\mathrm{c.m.}}(K) = \hbar^2 K^2/2m$ and $K_{\mathrm{rel}}(k) = \hbar^2 k^2/m$ for the kinetic energies of the c..m. and relative motion, respectively. The first term is the overall kinetic energy in a system of free particles counted by pairs. It can be rewritten in the usual way as

$$\sum_{p,\sigma}K(p)\hat{a}^\dagger_{\sigma,p}\hat{a}_{\sigma,p}, \quad (41)$$

where $K(p) = \hbar^2 p^2/2m$ is the standard kinetic energy matrix element. To see this, consider the configuration shown in Fig. 2. For the sake of transparency, we assume all pairs having $K = 0$. In this case $K_{\mathrm{rel}}(k) = K(k) + K(-k)$. We omit the corresponding index in the pair operators $\hat{C}_{\sigma\sigma',k,0} \equiv \hat{C}_{\sigma\sigma',k}$. The energy counting by using the first sum in the line (40) yields

$$\frac{1}{2}\sum_k K_{\mathrm{rel}}(k)\hat{C}^\dagger_{\uparrow\uparrow,k}\hat{C}_{\uparrow\uparrow,k} = \frac{1}{2}[K(q) + K(-q)]\times 2,$$

$$\frac{1}{2}\sum_k K_{\mathrm{rel}}(k)\hat{C}^\dagger_{\downarrow\downarrow,k}\hat{C}_{\downarrow\downarrow,k} = \frac{1}{2}[K(p) + K(-p)]\times 2,$$

$$\frac{1}{2}\sum_k K_{\mathrm{rel}}(k)\hat{C}^\dagger_{\uparrow\downarrow,k}\hat{C}_{\uparrow\downarrow,k} = \frac{1}{2}[K(k) + K(-k)]\times 1$$
$$+ \frac{1}{2}[K(k') + K(-k')]\times 1,$$

$$\frac{1}{2}\sum_k K_{\mathrm{rel}}(k)\hat{C}^\dagger_{\downarrow\uparrow,k}\hat{C}_{\downarrow\uparrow,k} = \frac{1}{2}[K(-k') + K(k')]\times 1$$
$$+ \frac{1}{2}[K(-k) + K(k)]\times 1. \quad (42)$$

The sum of the above results is identical to that obtained by using Eq. (41). The second sum in the line (40) yields the interaction energy accumulated in the scattering states. Consider the "$\sigma\bar{\sigma}$" channels. By using the relations (34) and the symmetry of the interaction potential with respect to the time reversal

$$V_{\uparrow\downarrow}(k'-k) = V_{\downarrow\uparrow}(-k'+k),$$

we write

$$\frac{1}{2S}\sum_{k'k}[V_{\uparrow\downarrow}(k'-k)\hat{C}^\dagger_{\uparrow\downarrow,k'}\hat{C}_{\uparrow\downarrow,k} + V_{\downarrow\uparrow}(k'-k)\hat{C}^\dagger_{\downarrow\uparrow,k'}\hat{C}_{\downarrow\uparrow,k}]$$
$$= \frac{1}{S}\sum_{k'k}V_{\uparrow\downarrow}(k'-k)\hat{C}^\dagger_{\uparrow\downarrow,k'}\hat{C}_{\uparrow\downarrow,k}.$$

By denoting $\hat{C}_{\uparrow\downarrow,k} \equiv \hat{b}_k$ and $V_{\uparrow\downarrow}(k'-k) \equiv V_{k'k}$ one gets the so-called *reduced Hamiltonian* employed by Bardeen, Cooper, and Schrieffer in their seminal work [33]:

$$\hat{H}_{\mathrm{red}} = \sum_k \frac{\hbar^2 k^2}{m}\hat{b}^\dagger_k\hat{b}_k + \frac{1}{S}\sum_{k'k}V_{k'k}\hat{b}^\dagger_{k'}\hat{b}_k.$$

Let us now consider the diagonal contribution due to the bound states. In the frame of our toy model introduced in Sec. II, the potential $V_{\uparrow\downarrow}(r)$ has a unique s-wave bound state. We denote the corresponding operator and the eigenvalue as $\hat{C}_{\uparrow\downarrow,1s,K} \equiv \hat{C}_{\uparrow\downarrow,K}$ and $\varepsilon_{1s} \equiv \varepsilon$, respectively. We make use of Eq. (35) and the relation (34) to obtain

$$\sum_K [K_{\mathrm{cm}}(K) + \varepsilon]\hat{C}^\dagger_{\uparrow\downarrow,K}\hat{C}_{\uparrow\downarrow,K}.$$

Next, we consider the off-diagonal terms. Start with the scattering states. By taking the nonzero matrix elements in the uppermost row and right column of the matrix presented in the left panel of Fig. 3 and using Eqs. (34) we get

$$-\sum_{k,K}\hbar\Omega(k+K/2)\cdot[s_{\uparrow\downarrow}(\hat{C}^\dagger_{\uparrow\uparrow,k,K}\hat{C}_{\downarrow\uparrow,k,K} + \hat{C}^\dagger_{\uparrow\downarrow,k,K}\hat{C}_{\downarrow\downarrow,k,K})$$
$$+ s_{\downarrow\uparrow}(\hat{C}^\dagger_{\downarrow\downarrow,k,K}\hat{C}_{\uparrow\downarrow,k,K} + \hat{C}^\dagger_{\downarrow\uparrow,k,K}\hat{C}_{\uparrow\uparrow,k,K})].$$

One can easily see that in terms of the particle operators this contribution is just the term describing SO coupling in the original Hamiltonian (1). Furthermore, by using the analogous matrix elements for the transitions involving the bound state (right panel in Fig. 3) we obtain

$$-\frac{1}{2}\sum_{k,K}\phi^*(k)\hat{C}^\dagger_{\uparrow\downarrow,K}[\hbar\Omega(-k+K/2)$$
$$- \hbar\Omega(k+K/2)]\cdot s_{\downarrow\uparrow}\hat{C}_{\uparrow\uparrow,k,K},$$

$$-\frac{1}{2}\sum_{k,K}\phi^*(k)\hat{C}^\dagger_{\uparrow\downarrow,K}[\hbar\Omega(k+K/2)$$
$$- \hbar\Omega(-k+K/2)]\cdot s_{\uparrow\downarrow}\hat{C}_{\downarrow\downarrow,k,K},$$

and their complex conjugation. In what follows, we shall use the shorthand notation $\hat{C}_{\uparrow\downarrow,0} \equiv \hat{C}_{\uparrow\downarrow}$ for the bound state

(ss)	$\lvert\uparrow\uparrow\rangle$	$\lvert\uparrow\downarrow\rangle$	$\lvert\downarrow\uparrow\rangle$	$\lvert\downarrow\downarrow\rangle$
$\langle\uparrow\uparrow\rvert$	$\left(\frac{\hbar^2K^2}{4m}+\frac{\hbar^2k^2}{m}\right)\delta_{\bar K K}\delta_{\bar k k}$ $-\mu_B gB\,\delta_{\bar K K}\delta_{\bar k k}$ $+V_{\uparrow\uparrow}(\bar k-k)\delta_{\bar K K}$	$-\hbar\bar\Omega\!\left(-\bar k+\frac{\bar K}{2}\right)\!\cdot s_{\uparrow\uparrow}\delta_{\bar K K}\delta_{\bar k k}$	$-\hbar\bar\Omega\!\left(\bar k+\frac{\bar K}{2}\right)\!\cdot s_{\uparrow\downarrow}\delta_{\bar K K}\delta_{\bar k k}$	0
$\langle\uparrow\downarrow\rvert$	$-\hbar\bar\Omega\!\left(-\bar k+\frac{\bar K}{2}\right)\!\cdot s_{\downarrow\uparrow}\delta_{\bar K K}\delta_{\bar k k}$	$\left(\frac{\hbar^2K^2}{4m}+\frac{\hbar^2k^2}{m}\right)\delta_{\bar K K}\delta_{\bar k k}$ $+V_{\uparrow\downarrow}(\bar k-k)\delta_{\bar K K}$	0	$-\hbar\bar\Omega\!\left(\bar k+\frac{\bar K}{2}\right)\!\cdot s_{\uparrow\uparrow}\delta_{\bar K K}\delta_{\bar k k}$
$\langle\downarrow\uparrow\rvert$	$-\hbar\bar\Omega\!\left(\bar k+\frac{\bar K}{2}\right)\!\cdot s_{\uparrow\uparrow}\delta_{\bar K K}\delta_{\bar k k}$	0	$\left(\frac{\hbar^2K^2}{4m}+\frac{\hbar^2k^2}{m}\right)\delta_{\bar K K}\delta_{\bar k k}$ $+V_{\downarrow\uparrow}(\bar k-k)\delta_{\bar K K}$	$-\hbar\bar\Omega\!\left(-\bar k+\frac{\bar K}{2}\right)\!\cdot s_{\uparrow\uparrow}\delta_{\bar K K}\delta_{\bar k k}$
$\langle\downarrow\downarrow\rvert$	0	$-\hbar\bar\Omega\!\left(\bar k+\frac{\bar K}{2}\right)\!\cdot s_{\uparrow\uparrow}\delta_{\bar K K}\delta_{\bar k k}$	$-\hbar\bar\Omega\!\left(-\bar k+\frac{\bar K}{2}\right)\!\cdot s_{\uparrow\uparrow}\delta_{\bar K K}\delta_{\bar k k}$	$\left(\frac{\hbar^2K^2}{4m}+\frac{\hbar^2k^2}{m}\right)\delta_{\bar K K}\delta_{\bar k k}$ $+\mu_B gB\,\delta_{\bar K K}\delta_{\bar k k}$ $+V_{\downarrow\downarrow}(\bar k-k)\delta_{\bar K K}$

(bs)	$\lvert\uparrow\uparrow\rangle$	$\lvert\uparrow\downarrow\rangle$	$\lvert\downarrow\uparrow\rangle$	$\lvert\downarrow\downarrow\rangle$
$\langle\uparrow\uparrow\rvert$	$\left(\frac{\hbar^2K^2}{4m}+\frac{\hbar^2k^2}{m}\right)\delta_{\bar K K}\delta_{\bar k k}$ $-\mu_B gB\,\delta_{\bar K K}\delta_{\bar k k}$ $+V_{\uparrow\uparrow}(\bar k-k)\delta_{\bar K K}$	$-\hbar\bar\Omega\!\left(-\bar k+\frac{\bar K}{2}\right)\!\cdot s_{\uparrow\uparrow}\phi(\bar k)\delta_{\bar K K}$	$-\hbar\bar\Omega\!\left(\bar k+\frac{\bar K}{2}\right)\!\cdot s_{\uparrow\downarrow}\phi(\bar k)\delta_{\bar K K}$	0
$\langle\uparrow\downarrow\rvert$	$-\hbar\bar\Omega\!\left(-\bar k+\frac{\bar K}{2}\right)\!\cdot s_{\downarrow\uparrow}\phi^*(\bar k)\delta_{\bar K K}$	$\left(\frac{\hbar^2K^2}{4m}+\varepsilon\right)\delta_{\bar K K}$	0	$-\hbar\bar\Omega\!\left(\bar k+\frac{\bar K}{2}\right)\!\cdot s_{\uparrow\uparrow}\phi^*(\bar k)\delta_{\bar K K}$
$\langle\downarrow\uparrow\rvert$	$-\hbar\bar\Omega\!\left(\bar k+\frac{\bar K}{2}\right)\!\cdot s_{\uparrow\uparrow}\phi^*(\bar k)\delta_{\bar K K}$	0	$\left(\frac{\hbar^2K^2}{4m}+\varepsilon\right)\delta_{\bar K K}$	$-\hbar\bar\Omega\!\left(-\bar k+\frac{\bar K}{2}\right)\!\cdot s_{\uparrow\uparrow}\phi^*(\bar k)\delta_{\bar K K}$
$\langle\downarrow\downarrow\rvert$	0	$-\hbar\bar\Omega\!\left(\bar k+\frac{\bar K}{2}\right)\!\cdot s_{\uparrow\uparrow}\phi(\bar k)\delta_{\bar K K}$	$-\hbar\bar\Omega\!\left(-\bar k+\frac{\bar K}{2}\right)\!\cdot s_{\uparrow\uparrow}\phi(\bar k)\delta_{\bar K K}$	$\left(\frac{\hbar^2K^2}{4m}+\frac{\hbar^2k^2}{m}\right)\delta_{\bar K K}\delta_{\bar k k}$ $+\mu_B gB\,\delta_{\bar K K}\delta_{\bar k k}$ $+V_{\downarrow\downarrow}(\bar k-k)\delta_{\bar K K}$

FIG. 3. The matrix elements $\mathcal{H}^{k'(n'),K',k(n),K}_{\sigma_1'\sigma_2'\sigma_1\sigma_2}$ involving the scattering states (ss) and the bound state (bs) of the four possible two-body scattering channels characterized by the orthogonal spin states $|\sigma\sigma'\rangle$. The $|\sigma\sigma\rangle$ channels involve only scattering states. The right panel (bs) shows the matrix elements between such states (i.e., 2D plane waves to the zeroth order in the corresponding scattering potentials) and the unique s-wave bound state of the $|\uparrow\downarrow\rangle$ (or, equivalently, $|\downarrow\uparrow\rangle$) channel. Formally, a combination of the $|\sigma\sigma\rangle$ spin state and the bound state wave function under the integral in Eq. (38) is allowed, but is excluded from the Hamiltonian by our definition of the relevant operator $\hat C_{\sigma_1\sigma_2,n,K}\equiv\delta_{\sigma_1\bar\sigma_2}\hat C_{\uparrow\downarrow,n,K}$ given below Eq. (37). The highlighted sector corresponds to the projected model employed in Sec. V.

operator with $K = 0$. We notice that for the effective SO fields of the type (7) or (8) one has

$$\tfrac{1}{2}[\boldsymbol{\Omega}(-\boldsymbol{k}+\boldsymbol{K}/2)-\boldsymbol{\Omega}(\boldsymbol{k}+\boldsymbol{K}/2)]=\boldsymbol{\Omega}^{(a)}(\boldsymbol{k}), \qquad (43)$$

so that the quantum amplitude linking the bound state to the scattering continua does not depend on the c.m. momentum $\boldsymbol{K}$. This interesting consequence of the Fermi statistics will prove to be useful for further consolidation of our formalism.

V. STRONG PAIRING AT HIGH MAGNETIC FIELDS

We now apply the above formalism to the problem of fermion pairing under SO coupling on the BEC side of the bare crossover. In the absence of the magnetic field and SO coupling we have a spin-singlet scattering channel including the corresponding continuum and a bound state, and three degenerate channels belonging to the spin triplet. The magnetic field splits the triplet with the "↑↑" channel going to the bottom. We are particularly interested in the situation where $|\varepsilon+\mu_B gB|\ll\mu_B gB$. In this case we may neglect coupling to the $S_z=0,-1$ scattering states and obtain the following

(grand canonical) model:

$$
\begin{aligned}
\hat H &= \frac{1}{2}\sum_{\boldsymbol{k}}\left(\frac{\hbar^2 k^2}{m}-\mu_B gB-2\mu\right)\hat C^{\dagger}_{\uparrow\uparrow,\boldsymbol{k}}\hat C_{\uparrow\uparrow,\boldsymbol{k}} \\
&\quad+(\varepsilon-2\mu)\hat C^{\dagger}_{\uparrow\downarrow}\hat C_{\uparrow\downarrow}+\frac{1}{2S}\sum_{\boldsymbol{k}',\boldsymbol{k}}V_{\uparrow\uparrow}(\boldsymbol{k}'-\boldsymbol{k})\hat C^{\dagger}_{\uparrow\uparrow,\boldsymbol{k}'}\hat C_{\uparrow\uparrow,\boldsymbol{k}} \\
&\quad-\sum_{\boldsymbol{k}}\hbar\boldsymbol{\Omega}^{(a)}(\boldsymbol{k})\cdot[s_{\uparrow\downarrow}\phi(\boldsymbol{k})\hat C^{\dagger}_{\uparrow\uparrow,\boldsymbol{k}}\hat C_{\uparrow\downarrow}+\mathrm{H.c.}].
\end{aligned}
$$
$$(44)$$

The last term describes the coherent SO coupling between the bound state and the continuum of scattering states in the "↑↑" channel, and has the form anticipated on the basis of general arguments given in Sec. IV A and our analysis of the BCS limit in Sec. III.

A. Two-body scattering in vacuum

In vacuum the following commutation relations hold for the fermion pair operators:

$$
\begin{aligned}
[\hat C_{\sigma\sigma,\boldsymbol{k}'},\hat C^{\dagger}_{\sigma\sigma,\boldsymbol{k}}] &= \pm\delta_{\boldsymbol{k}',\pm\boldsymbol{k}}, \\
[\hat C_{\uparrow\downarrow,\boldsymbol{K}'},\hat C^{\dagger}_{\uparrow\downarrow,\boldsymbol{K}}] &= \delta_{\boldsymbol{K}',\boldsymbol{K}}.
\end{aligned}
$$
$$(45)$$

By using the Hamiltonian (44) with $\mu\equiv 0$ one may then obtain the following Heisenberg equations of motion:

$$i\hbar\frac{d}{dt}\hat C_{\uparrow\uparrow,\boldsymbol{k}}=\left(\frac{\hbar^2 k^2}{m}-\mu_B gB\right)\hat C_{\uparrow\uparrow,\boldsymbol{k}}+\frac{1}{S}\sum_{\boldsymbol{k}'}V_{\uparrow\uparrow}(\boldsymbol{k}'-\boldsymbol{k})\hat C_{\uparrow\uparrow,\boldsymbol{k}'}-2\hbar\boldsymbol{\Omega}^{(a)}(\boldsymbol{k})\cdot s_{\uparrow\downarrow}\phi(\boldsymbol{k})\hat C_{\uparrow\downarrow}, \qquad (46\mathrm{a})$$

$$i\hbar\frac{d}{dt}\hat C_{\uparrow\downarrow}=\varepsilon\hat C_{\uparrow\downarrow}-\sum_{\boldsymbol{k}}\hbar\boldsymbol{\Omega}^{(a)}(\boldsymbol{k})\cdot s_{\downarrow\uparrow}\phi^*(\boldsymbol{k})\hat C_{\uparrow\uparrow,\boldsymbol{k}}. \qquad (46\mathrm{b})$$

We make the substitution

$$\hat{C}_{\uparrow\uparrow,\boldsymbol{k}}(t) \rightarrow \sum_{\boldsymbol{q}} \psi_{\boldsymbol{q}}^{(+)}(\boldsymbol{k})\hat{C}_{\uparrow\uparrow,\boldsymbol{q}}^{(+)}e^{-i(E_k-\mu_B gB+i0)t/\hbar}, \quad (47a)$$

$$\hat{C}_{\uparrow\downarrow}(t) \rightarrow \hat{C}_{\uparrow\downarrow}e^{-i(E_k-\mu_B gB)t/\hbar} \quad (47b)$$

with the standard notation $E_k \equiv \hbar^2 k^2/m$ for the kinetic energy of the relative motion, eliminate $\hat{C}_{\uparrow\downarrow}$ from Eq. (46a) in favor of $\hat{C}_{\uparrow\uparrow,\boldsymbol{k}}(t)$, and replace the sums by integrals according to the standard rule

$$\sum_{\boldsymbol{k}} \rightarrow \frac{S}{(2\pi)^2}\int d\boldsymbol{k}. \quad (48)$$

It will also be convenient to count the energy from the bottom band by introducing the detuning

$$\bar{\delta} \equiv \varepsilon + \mu_B gB. \quad (49)$$

This way, we arrive at the Lippman-Schwinger equation

$$|\boldsymbol{q}+\rangle = |\boldsymbol{q}+\rangle_{\text{bg}}$$
$$+ G_{\uparrow\uparrow}^0(E_q+i0)\Omega^\dagger G_{\uparrow\downarrow}(E_q)\Omega|\boldsymbol{q}+\rangle \quad (50)$$

for the stationary scattering state $\psi_{\boldsymbol{q}}^{(+)}(\boldsymbol{k}) = \langle \boldsymbol{k}|\boldsymbol{q}+\rangle$ in the $S_z = +1$ (open) channel. Here

$$|\boldsymbol{q}+\rangle_{\text{bg}} = |\boldsymbol{q}\rangle + G_{\uparrow\uparrow}^0(E_q+i0)V_{\uparrow\uparrow}|\boldsymbol{q}+\rangle_{\text{bg}} \quad (51)$$

describes distortion of the wave function by the background potential $V_{\uparrow\uparrow}(\boldsymbol{r})$,

$$G_{\uparrow\uparrow}^0(z) = (z - K_{\text{rel}})^{-1}, \quad (52a)$$

$$G_{\uparrow\downarrow}(E) = \frac{|\varphi\rangle\langle\varphi|}{E-\delta} \quad (52b)$$

are the Green's operators of the (free) relative motion in the open-channel and the closed-channel bound state $|\varphi\rangle$, respectively, and we have defined

$$\Omega \equiv \sqrt{2}\int \hbar\boldsymbol{\Omega}^{(a)}(\boldsymbol{k})\cdot \boldsymbol{s}_{\uparrow\downarrow}|\boldsymbol{k}\rangle\langle\boldsymbol{k}|\,d\boldsymbol{k}. \quad (53)$$

As usual, we are interested in the low-energy scattering $E_q \rightarrow 0$. For our illustrative purposes, we may safely put $|\boldsymbol{q}+\rangle_{\text{bg}} \equiv |\boldsymbol{q}\rangle$ in this case.[1] By using the relation

$$|\boldsymbol{q}+\rangle = |\boldsymbol{q}\rangle + G_{\uparrow\uparrow}^0(E_q+i0)T_{\uparrow\uparrow}(E_q+i0)|\boldsymbol{q}\rangle \quad (54)$$

one may obtain from Eq. (50)

$$T_{\uparrow\uparrow} = V_{\uparrow\uparrow}^{(\text{eff})}(E) + V_{\uparrow\uparrow}^{(\text{eff})}(E)G_{\uparrow\uparrow}^0 T_{\uparrow\uparrow}, \quad (55)$$

where

$$V_{\uparrow\uparrow}^{(\text{eff})}(E) = \Omega^\dagger G_{\uparrow\downarrow}(E)\Omega. \quad (56)$$

By expanding Eq. (55) into an infinite geometrical series and summing it up, we find

$$\langle\boldsymbol{k}'|T_{\uparrow\uparrow}(E_k+i0)|\boldsymbol{k}\rangle = \frac{\langle\boldsymbol{k}'|\Omega^\dagger|\varphi\rangle D(E_k)\langle\varphi|\Omega|\boldsymbol{k}\rangle}{1 - \Pi(E_k+i0)D(E_k)} \quad (57)$$

──────────

[1] In principle, one may show that, quite generically, the contribution of the background potential $V_{\uparrow\uparrow}(\boldsymbol{r})$ is negligible in 2D.
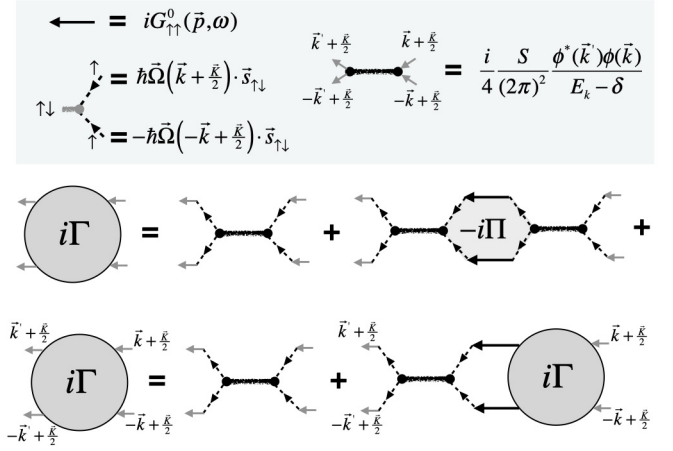

FIG. 4. Four-leg vertex function for the scattering of two fermions in vacuum. The topmost inset shows the dictionary used to construct the graphs. An unconventional element is the SO coupling of a pair of spin-↑ fermion lines (solid arrows) to the molecular propagator (smashed line) represented by a pair of dashed lines. Each of these connecting lines can be regarded as an effective field acting in the spin subspace. The antisymmetrization of the molecular spin state is accomplished by ascribing opposite signs to the corresponding spin-flip amplitudes. The two processes add up to produce the antisymmetrized effective field $\boldsymbol{\Omega}^{(a)}(\boldsymbol{k})$ [Eq. (14)] that does not depend on the c.m. momentum $\boldsymbol{K}$. This makes possible the usual identification of the vertex $\Gamma_{\uparrow\uparrow\uparrow\uparrow}(\boldsymbol{k}',\boldsymbol{k},\boldsymbol{K},E_k)$ with the two-body scattering T matrix $T_{\uparrow\uparrow}(\boldsymbol{k}',\boldsymbol{k},E_k+i0)$.

with

$$\Pi(z) = \int d\boldsymbol{q}\,\frac{\langle\varphi|\Omega|\boldsymbol{q}\rangle\langle\boldsymbol{q}|\Omega^\dagger|\varphi\rangle}{z-E_q} \quad (58)$$

and $D(E) \equiv \langle\varphi|G_{\uparrow\downarrow}(E)|\varphi\rangle$.

In terms of the four-leg vertex function $\Gamma_{\uparrow\uparrow\uparrow\uparrow}(\boldsymbol{k}',\boldsymbol{k},\boldsymbol{K},E_k)$, the above result can be expressed by introducing momentum-dependent connecting (dashed) lines between the single-fermion lines and the molecular propagator in the corresponding Bethe-Salpeter equation (Fig. 4). In the absence of two-body interaction, such lines would realize dressing of the spin-↑ fermions with their spin-↓ partners due to the SO coupling. In the two-particle picture, they connect the scattering states in the spin-triplet and -singlet scattering channels. Appearance of the tightly bound state in the singlet channel due to the attractive interaction $V_{\uparrow\downarrow}(\boldsymbol{r})$ allows one to neglect the SO coupling to the higher-energy scattering states of the same channel and consider only coupling of the bare spin-↑ fermion lines with $\boldsymbol{p}_{1,2} = \pm\boldsymbol{k} + \boldsymbol{K}/2$ to the molecular propagator. Antisymmetrization of the molecular spin state requires that we add up the corresponding amplitudes with opposite signs. As a result, one gets the antisymmetrized effective field $\boldsymbol{\Omega}^{(a)}(\boldsymbol{k})$ [Eq. (14)] that does not depend on the c.m. momentum $\boldsymbol{K}$. The vertex function $\Gamma_{\uparrow\uparrow\uparrow\uparrow}(\boldsymbol{k}',\boldsymbol{k},\boldsymbol{K},E_k)$ is then $\boldsymbol{K}$ independent as well and can be readily identified with the two-body scattering T matrix given by Eq. (55):

$$\Gamma_{\uparrow\uparrow\uparrow\uparrow}(\boldsymbol{k}',\boldsymbol{k},E_k) = (2\pi)^2 T_{\uparrow\uparrow}(\boldsymbol{k}',\boldsymbol{k},E_k+i0). \quad (59)$$

By virtue of the relationship (14) the antisymmetry of the fermion vertex (59) with respect to the exchange of the two outgoing legs ($k' \rightarrow -k'$) is ensured automatically.

To proceed, let us make some explicit choices for the main ingredients of our model. A natural form of the pair wave function in the strong-pairing regime is the Gaussian ansatz

$$|\langle \mathbf{k}|\varphi\rangle|^2 = \frac{a^2}{\pi}e^{-(ka)^2}, \qquad (60)$$

the microscopic radius a thus setting an ultraviolet cutoff for our low-energy theory. The Gaussian ansatz has been widely used in the BCS-BEC crossover problem [20]. Evaluation of the pair polarization bubble (58) by using the Rashba expression (8) for the SO field then yields

$$\Pi(E_k + i0) = -\frac{m\upsilon_R^2}{2}[1 - e^{-x}x\,\mathrm{Ei}(x) - i\pi e^{-x}x] \qquad (61)$$

with $E_a = \hbar^2/ma^2$, $x \equiv E_k/E_a$, and $\mathrm{Ei}(x)$ being the exponential integral [34]. By substituting the low-energy expansion of this result into Eq. (55) one may obtain the on-shell 2D scattering amplitude for two spin-↑ fermions in vacuum $f_{\uparrow\uparrow,\mathbf{k}'}(\mathbf{k}) = -(2\pi)^2 m/2\hbar^2\,\langle \mathbf{k}'|\,T_{\uparrow\uparrow}(E_k + i0)\,|\mathbf{k}\rangle$:

$$f_{\uparrow\uparrow,\mathbf{k}'}(\mathbf{k}) = -\frac{2\pi e^{i(\theta'-\theta)}}{\frac{E_k-\delta}{\beta E_k/E_a} + \ln(E_a e^{-\gamma}/E_k) + i\pi}, \qquad (62)$$

where $\beta = m\upsilon_R^2/2$, $\delta = \bar{\delta} - \beta$, γ is the Euler-Mascheroni constant, and $E_a = \hbar^2/ma^2$. The scattering amplitude has the genuine p-wave form. Being considered as a complex function of the energy E it has a pole at

$$\tilde{E} = \tilde{\delta} + \tilde{\beta}\tilde{E}\,\ln(\tilde{E}e^{\gamma}) - i\pi\tilde{\beta}\tilde{E}, \qquad (63)$$

where we have adopted the dimensionless quantities $\tilde{E} \equiv E/E_a$, etc. This pole is a p-wave resonance at positive detuning $\delta > 0$ and a bound state of the two-channel Hamiltonian (44) at $\delta < 0$. In the relevant regime

$$\tilde{\beta} = \beta/E_a \ll 1 \qquad (64)$$

the resonance is narrow. The significance of this observation will be clarified later. The position of the resonance is shifted toward lower energies with respect to the bare bound state level ε by the amount β. By recasting the bare detuning (49) in the form $\bar{\delta} = \mu_B g(B - B_0)$ and, consistently, $\delta = \mu_B g(B - B_c)$ with

$$B_c = B_0 + \beta/\mu_B g, \qquad (65)$$

we plot schematically in Fig. 5 the (real) energy E of the pole as a function of the magnetic field B over the whole range. At $B \ll B_c$ and $B \gg B_c$ the function $E(B)$ approaches the asymptote $E(B) = \mu_B g(B - B_0)$ (dashed line). In the narrow resonance limit (64) one has $E(0) = \varepsilon$. The most interesting phenomenon occurs at $B \rightarrow B_c$, where the derivative

$$\frac{\partial E}{\partial B} = -\frac{\mu_B g}{\tilde{\beta}\,\ln \tilde{E}} \qquad (66)$$

slowly approaches 0. A synthetic p-wave halo emerging from the nominally s-wave bound state in this limit is the subject of the next subsection.
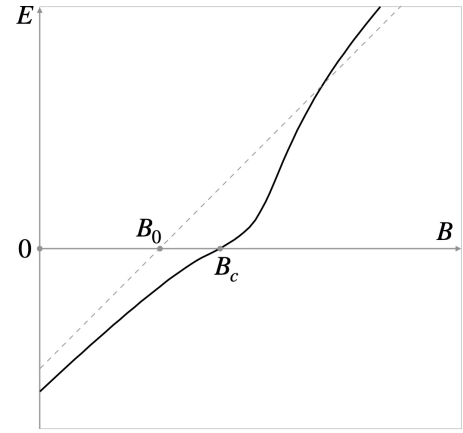

FIG. 5. The pole E of the scattering amplitude $f_{\uparrow\uparrow,\mathbf{k}'}(\mathbf{k})$ as a function of the magnetic field B. The full equation (61) for the pair polarization bubble with $\tilde{\beta} = 0.5$ has been used. At $B > B_c$ only the real part of E is shown. The dashed line indicates the asymptote $E(B) = \mu_B g(B - B_0)$. In the adopted scale the slow logarithmic running of the tangent slope $\partial E/\partial B$ toward 0 at $B \rightarrow B_c$ is not discernible.

B. Synthetic p-wave halo

Let us write the relative motion Hamiltonian $\mathcal{H}_{\mathrm{rel}}$ which can be used to obtain the truncated second-quantized version (44) following the standard prescription

$$\hat{H} = \langle \hat{\Psi}|\,\mathcal{H}_{\mathrm{rel}}\,|\hat{\Psi}\rangle \qquad (67)$$

with $\langle \hat{\Psi}| = (\langle \hat{\psi}_{\uparrow\uparrow}|, \langle \hat{\varphi}|)$, where the two components are the projections onto $|\uparrow\uparrow\rangle$ and $|m\rangle = \frac{1}{\sqrt{2}}(|\uparrow\downarrow\rangle - |\downarrow\uparrow\rangle)$ in the pair spin subspace. The molecular field operator is just $|\hat{\varphi}\rangle = \hat{C}_{\uparrow\downarrow}|\varphi\rangle$. By noticing that the normalization relation for the open-channel pair operators can be recast as

$$\hat{N}_{\uparrow\uparrow} \equiv \langle \hat{\psi}_{\uparrow\uparrow}|\hat{\psi}_{\uparrow\uparrow}\rangle = \frac{1}{2}\sum_{k}\hat{C}^{\dagger}_{\uparrow\uparrow,k}\hat{C}_{\uparrow\uparrow,k}, \qquad (68)$$

we conclude that the proper expansion of $\hat{\psi}_{\uparrow\uparrow}(\mathbf{r}) = \langle \mathbf{r}|\hat{\psi}_{\uparrow\uparrow}\rangle$ in terms of $\hat{C}_{\uparrow\uparrow,\mathbf{k}}$ should read as

$$\hat{\psi}_{\uparrow\uparrow}(\mathbf{r}) = \frac{1}{\sqrt{2S}}\sum_{k}\hat{C}_{\uparrow\uparrow,k}e^{i\mathbf{k}\mathbf{r}}. \qquad (69)$$

We thus find

$$\mathcal{H}_{\mathrm{rel}} = \begin{pmatrix} K_{\mathrm{rel}} + V_{\uparrow\uparrow} & \Omega \\ \Omega^{\dagger} & \bar{\delta}\,|\varphi\rangle\,\langle\varphi| \end{pmatrix}, \qquad (70)$$

where the operator Ω is given by Eq. (53). This form may also be seen to provide the highlighted sector of the matrix Hamiltonian shown in Fig. 3.

The relative motion Hamiltonian (70) possesses a synthetic bound state corresponding to the real negative pole (63) of the scattering amplitude $f_{\uparrow\uparrow,\mathbf{k}'}(\mathbf{k})$ found in Sec. V A. The two-component wave function

$$|\Phi\rangle = \begin{pmatrix} |\phi_{\uparrow\uparrow}\rangle \\ |\phi\rangle \end{pmatrix} \qquad (71)$$

of this state is a solution of the eigenvalue problem with $E < 0$:

$$(K_{\rm rel} + V_{\uparrow\uparrow}) |\phi_{\uparrow\uparrow}\rangle + \Omega |\phi\rangle = E |\phi_{\uparrow\uparrow}\rangle, \qquad (72a)$$

$$\Omega^\dagger |\phi_{\uparrow\uparrow}\rangle + \bar\delta |\varphi\rangle \langle\varphi|\phi\rangle = E |\phi\rangle. \qquad (72b)$$

By using Eqs. (52) we obtain

$$|\Phi\rangle = \frac{1}{\sqrt{1 + \langle\varphi| \Omega^\dagger G_{\uparrow\uparrow}^2(E)\Omega |\varphi\rangle}} \begin{pmatrix} G_{\uparrow\uparrow}(E)\Omega |\varphi\rangle \\ |\varphi\rangle \end{pmatrix}.$$

One can easily sea that

$$\langle\varphi| \Omega^\dagger G_{\uparrow\uparrow}^2(E)\Omega |\varphi\rangle = -\frac{\partial \Pi(E)}{\partial E},$$

where $\Pi(E)$ is given by Eq. (58). On the other hand, $\Pi(E) = E - \bar\delta$. We thus obtain that the quantity

$$w^2 = (\mu_B g)^{-1} \frac{\partial E}{\partial B} \qquad (73)$$

defines the relative weight of the bare bound state wave function in the composite state $|\Phi\rangle$. According to Eq. (66), $w \to 0$ as $B \to B_c$.

In real space the composite state $|\Phi\rangle$ can be written as

$$\langle r|\Phi\rangle = |\uparrow\uparrow\rangle \, \Upsilon(r) + \frac{1}{\sqrt 2}(|\uparrow\downarrow\rangle - |\downarrow\uparrow\rangle) w\varphi(r), \qquad (74)$$

where $\Upsilon(r)$ represents the wave function of the so-called *quantum halo* [35]: A superposition of the continuum states in the open channel due to coherent disintegration of the bare molecule. The halo extends far beyond the tightly bound core and carries an orbital angular momentum $L_z = -\hbar$. Thus, for the Gaussian ansatz (60) at $B \to B_c$ we obtain

$$\Upsilon(r) = \frac{w}{\sqrt{2\pi}} \frac{m\upsilon_R}{\hbar} \frac{a}{r}(1 - e^{-r^2/2a^2})e^{-i\alpha}, \qquad (75)$$

where r and α are the polar coordinates of the radius vector r. Note that the logarithmic attenuation of w at the resonance is compensated by the slow $1/r$ decay of the wave function (75) at large distances, so that

$$2\pi \int_0^\lambda |\Upsilon(r)|^2 r\, dr \to 1 \qquad (76)$$

as $\lambda \sim \sqrt{\hbar/2mE} \to \infty$ and the total probability is transferred from the core to the halo.

The energy $E(B)$ defined by Eq. (63) should not be confused with the dissociation energy of the molecule. The synthetic wave function (74) itself represents a partially disintegrated state, the halo being quantum superposition of the continuum states in the open channel. Destruction of the correlations responsible for the halo occurs when the thermal energy $k_B T$ becomes comparable with the energy of the coherent SO link between the channels, the latter being on the order of $\hbar\upsilon_R/a$. For the Bi2212 cuprate supreconductor where signatures of strong SO coupling have recently been reported [36], we estimate the corresponding temperature to be several tens of K, which is comparable with the critical temperature of such systems.

C. Topological BCS-BEC phase transition

The performed second quantization in the basis of pair states grants an insight into the collective behavior of the strongly paired SO coupled fermions in the vicinity of B_c. Let us rewrite the Hamiltonian in terms of the familiar single-fermion creation and annihilation operators $\hat a_{\sigma,\boldsymbol{p}}^\dagger$ and $\hat a_{\sigma,\boldsymbol{p}}$, keeping only the molecular operators $\hat C_{\uparrow\downarrow}^\dagger$ and $\hat C_{\uparrow\downarrow}$. Following the considerations presented in Sec. IV C we obtain

$$\begin{aligned}
\hat H = & \sum_{\boldsymbol{k}} \left(\frac{\hbar^2 k^2}{2m} - \frac{1}{2}\mu_B g B - \mu \right) \hat a_{\uparrow,\boldsymbol{k}}^\dagger \hat a_{\uparrow,\boldsymbol{k}} \\
& + (\varepsilon - 2\mu)\hat C_{\uparrow\downarrow}^\dagger \hat C_{\uparrow\downarrow} \\
& + \frac{1}{2S} \sum_{\boldsymbol{k},\boldsymbol{k}'} \hat a_{\uparrow,\boldsymbol{k}'}^\dagger \hat a_{\uparrow,-\boldsymbol{k}'}^\dagger V_{\uparrow\uparrow}(\boldsymbol{k}' - \boldsymbol{k}) \hat a_{\uparrow,-\boldsymbol{k}} \hat a_{\uparrow,\boldsymbol{k}} \\
& - \sum_{\boldsymbol{k}} \hbar\boldsymbol{\Omega}^{(a)}(\boldsymbol{k}) \cdot [\boldsymbol{s}_{\downarrow\uparrow}\phi^*(\boldsymbol{k})\hat C_{\uparrow\downarrow}^\dagger \hat a_{\uparrow,-\boldsymbol{k}} \hat a_{\uparrow,\boldsymbol{k}} + {\rm H.c.}].
\end{aligned}$$
$$(77)$$

Just like the weakly paired BCS model under the magnetic field and SO coupling has been shown to map onto a spinless (i.e., one-component) *p*-wave BCS superfluid [6] [see Sec. III and Eq. (17)], we find that the strongly paired molecular BEC at $B \to B_c$ maps onto a spinless *resonant p*-wave superfluid. The Hamiltonian (77) is the so-called Fano-Anderson model [27,28] successfully employed for investigation of ultracold Fermi gases with Feshbach-resonant interactions [31]. The role of the coherent Feshbach link in our case belongs to the SO coupling. In contrast to the BCS side of the *bare* crossover discussed in Sec. III, here both weak- and strong-pairing regimes are accessible upon variation of the magnetic field across B_c. The effectively broken time-reversal symmetry and *p*-wave-like momentum dependence of the coherent coupling between the channels render that latter crossover a canonical *topological phase transition* [17]. Again, this transition has also been extensively discussed in the literature [18,31,37].

The obtained mapping (77) in its own right should, therefore, be regarded as an important insight into the problem under consideration and the main result of our paper. Here, we shall only sketch a straightforward way to proceed with the many-body treatment of Eq. (77) by using the standard Bogoliubov prescription. For simplicity, we neglect the repulsive background potential $V_{\uparrow\uparrow}(r)$ and assume zero temperature. The bound pairs then form a Bose-Einstein condensate and the corresponding operator may be replaced by a *c*-number

$$\hat C_{\uparrow\downarrow} \to C_{\uparrow\downarrow} \qquad (78)$$

with $|C_{\uparrow\downarrow}|^2 = N/2$, N being the total (even) number of the condensed fermions. We are interested in the in-medium pair wave function (19) which can be expressed via the Bogoliubov coefficients $u_{\uparrow,\boldsymbol{k}}$ and $\upsilon_{\uparrow,\boldsymbol{k}}$ by Eq. (20), where we should substitute the gap Δ_{--} by

$$\hbar\boldsymbol{\Omega}^{(a)}(\boldsymbol{k}) \cdot \boldsymbol{s}_{\uparrow\downarrow}\phi(\boldsymbol{k})C_{\uparrow\downarrow} \approx \frac{\hbar\upsilon_R a}{2\sqrt\pi} C_{\uparrow\downarrow} ike^{-i\theta}$$

at low $\boldsymbol{k}$ and put $\hbar\omega(\boldsymbol{p}) = \mu_B g B$ in the definition of the quasiparticle energy (13). As before, we have assumed Eq. (8) for the effective SO field $\boldsymbol{\Omega}(\boldsymbol{k})$ and used the Gaussian ansatz (60).

For $-\mu_B g B < 2\mu < \varepsilon$ we recover the long-distance behavior obtained in Sec. III for the BCS regime:

$$g_{\uparrow\uparrow}(\boldsymbol{r}) \propto \sqrt{N}\frac{e^{-i\alpha}}{r}, \tag{79}$$

which we can now associate directly with the analogous asymptote for the quantum halo (75) in vacuum. Hence, the Cooper pairs possess *synthetic angular momenta*. The Pfaffian

$$\mathrm{Pf}\left(\frac{1}{z_i - z_j}\right) \tag{80}$$

with $z_i = x_i + i y_i$ defines the long-distance behavior of the many-body wave function $\Psi(\boldsymbol{r}_1, \ldots, \boldsymbol{r}_N)$. Being multiplied by the composite-fermion "tail" carrying two vortices it becomes the Moore-Read state for the filling factor $\frac{5}{2}$ in the FQHE [17].

As μ hits $\varepsilon/2$, the Cooper pairs start to convert into the tightly bound molecules of the pairing potential $V_{\uparrow\downarrow}(r)$. From now on, the chemical potential μ is pinned to the discrete level $\varepsilon/2$ and a regime $2\mu \leqslant -\mu_B g B$ can be reached. This should be contrasted with Sec. III. The pair wave function $g_{\uparrow\uparrow}(\boldsymbol{r})$ now decays exponentially. At the point $2\mu = -\mu_B g B$ the excitation spectrum is gapless and the Bogoliubov coefficients $u_{\uparrow,\boldsymbol{k}}$ and $v_{\uparrow,\boldsymbol{k}}$ considered as a map from the $\boldsymbol{k}$ space to the space of two real parameters[2] change their so-called homotopy class. A topological phase transition takes place.

A transition of this kind has already been anticipated in an earlier numerical study [11] and the linear scaling of the critical field B_c with the binding energy $|\varepsilon|$ has been reported. Our conclusions are in line with those results. The coexistence region interpreted in terms of an interplay between the population imbalance and SO coupling [38] may tentatively be associated with the resonant BCS-BEC crossover at $\varepsilon = 2\mu > -\mu_B g B$ in our approach (not to be confused with the *bare* crossover specified in Sec. II). In the course of such crossover the topologically nontrivial Cooper pair condensate coexists with the molecular BEC.

A noteworthy qualitative difference of the model (77) from the analogous constructions employed for genuine *p*-wave superfluids [31] is the synthetic origin of the angular momentum. The bare molecules are *s* wave. Hence, the topological BCS-BEC transition is accompanied by suppression of the "pseudorotation" of the condensate. According to Sec. V B, on the BEC side the angular momentum may persist due to the quantum halos in the immediate vicinity of B_c. It is an interesting open question if the critical (quantum) fluctuations may render the behavior of the synthetic angular momentum first order.

Finally, we note that the model (77) becomes particularly useful in the narrow resonance limit (64) where one may expect an arbitrarily accurate perturbative solution controlled by powers of the small parameter $\tilde{\beta}$ [31].

D. Relation to the projected BCS model

We would like to compare the Hamiltonian (44) with Eqs. (12) and (17) obtained in the weak-pairing limit. By using Eq. (35) for the molecular operator $\hat{C}_{\uparrow\downarrow}$ we may identify

---

[2]We recall that $|u_{\uparrow,\boldsymbol{k}}|^2 + |v_{\uparrow,\boldsymbol{k}}|^2 = 1$ and only the relative phase of $u_{\uparrow,\boldsymbol{k}}$ and $v_{\uparrow,\boldsymbol{k}}$ matters.

the second term in Eq. (44) with the weak attraction due to the separable force (9):

$$\epsilon \equiv \varepsilon, \tag{81a}$$

$$\chi(k) \equiv \phi(k). \tag{81b}$$

With this identification the (positive) shift of the scattering threshold in the singlet channel with respect to the lower-energy triplet channel induced by the Zeeman splitting amounts to the replacement $\epsilon \to \bar{\delta}$. We set $V_{\uparrow\uparrow}(r) \equiv 0$ and write the Hamiltonian (44) in the form

$$\hat{H} = \hat{H}_{\mathrm{BCS}}^{(\uparrow\uparrow)} + (\bar{\delta} - 2\mu)\hat{C}_{\uparrow\downarrow}^\dagger \hat{C}_{\uparrow\downarrow} \tag{82}$$

with

$$
\hat{H}_{\mathrm{BCS}}^{(\uparrow\uparrow)} = \frac{1}{2}\sum_{\boldsymbol{k}}\left(\frac{\hbar^2 k^2}{m} - 2\mu\right)\hat{C}_{\uparrow\uparrow,\boldsymbol{k}}^\dagger \hat{C}_{\uparrow\uparrow,\boldsymbol{k}}
$$
$$
- \sum_{\boldsymbol{k}}\hbar\boldsymbol{\Omega}^{(a)}(\boldsymbol{k})\cdot\boldsymbol{s}_{\uparrow\downarrow}\phi(k)\hat{C}_{\uparrow\uparrow,\boldsymbol{k}}^\dagger \hat{C}_{\uparrow\downarrow} - \mathrm{H.c.} \tag{83}
$$

In the BCS limit the detuning $\bar{\delta}$ [Eq. (49)] is positive and large, i.e., $\bar{\delta} \approx \mu_B g B \gg |\varepsilon|$. One can then easily see that the second term in Eq. (83) is identical to the anomalous part in Eq. (17). The first term in Eq. (83) is just the kinetic energy in the lowest single-particle band (see Sec. IV C). This way, we identify the Hamiltonian $\hat{H}_{\mathrm{BCS}}^{(\uparrow\uparrow)}$ with the projected BCS model $\hat{H}_{\mathrm{BCS}}^{(--)}$.

Furthermore, we may take advantage of Eq. (46b) to eliminate the molecular operator $\hat{C}_{\uparrow\downarrow}$ in favor of the free-pair operator $\hat{C}_{\uparrow\uparrow,\boldsymbol{k}}$ from Eq. (82). We obtain the first line in Eq. (12) and our argument on the effective *p*-wave attraction represented by Eq. (16) follows immediately.

The form (82) also suggests different origins of the pairing instability at $\mu_B g B \gg |\varepsilon|$ as compared to the $B \to 0$ limit of Eq. (21) considered in the earlier works [1]. In that latter case the instabilities in the SO-split chiral bands are due to the usual mechanical attraction $V_{\uparrow\downarrow}(r)$ between the $\boldsymbol{k}$ and $-\boldsymbol{k}$ fermions with opposite spins pointing along the effective fields shown in Fig. 1. In the frame of the Fano-Anderson model (82), in contrast, the effective attraction is due to the virtual spin flips linking the spin-$\uparrow$ polarized continuum to the far-positively detuned discrete level.

E. Experimental implementation

Recently, convincing arguments in favor of the BEC-BCS crossover phenomenology have been provided for high-temperature cuprate superconductors [30]. In the frame of the model (1) the cuprates seem to be in the strong-pairing BEC regime. Spin and angle-resolved photoemission spectroscopy (ARPES) of the prototypical Bi2212 ($Bi_2Sr_2CaCu_2O_8$) sample has revealed spin textures in the Brillouin zone [36] akin to the Rashba-type arrangement of the SO field shown in Fig. 1. We suggest, therefore, that the cuprates may naturally realize the strong fermionic pairing under SO coupling touched upon in our work. A challenging issue beyond our generic consideration would be an interplay of the Zeeman splitting comparable with the binding energy (on the order of the characteristic "pseudogap" temperature) and the antiferromagnetic order specific for such systems.

The dilute and even mesoscopic regime of the Fano-Anderson model (77) may potentially be implemented with

the ultracold atoms under the synthetic SO coupling. The time-of-flight technique [39] in combination with the spin-injection spectroscopy [40] could provide access to all key characteristics of the synthetic p-wave halo and resonance. These are the presence of the orbital momentum, the unique nonlinear dependence of the energy E on the magnetic field B shown in Fig. 5 [compare with the linear growth of $E(B)$ measured in a 3D sample [39]], the linear scaling of the resonance width with E (as opposed to the $\propto E^{3/2}$ dependence in 3D [39]) and the mixed spin structure of the state (74). Besides, high-resolution fluorescence measurements recently applied to a quasi-2D Fermi gas [41] could be used to image the halo wave function (75). The pristine Rashba form of the SO coupling (8), however, yet remains to be achieved in a 2D atomic setting [24].

VI. SUMMARY AND OUTLOOK

We have proposed an alternative formulation of the problem of 2D fermion pairing under SO coupling in terms of the second-quantized pair Hamiltonian. In this picture the effective SO field performs coherent switching between the two-body scattering channels labeled by the projection of the pair spin S_z. For a spin-singlet bound state interference of the quantum amplitudes for $\boldsymbol{k}$ and $-\boldsymbol{k}$ produces a Feshbach-type decay governed by the antisymmetric field $\boldsymbol{\Omega}^{(a)}(\boldsymbol{k})$ [Eq. (14)]. For the physically relevant Dresselhaus [Eq. (7)] or Rashba [Eq. (8)] types of SO coupling the field $\boldsymbol{\Omega}^{(a)}(\boldsymbol{k})$ does not depend on the c.m. momentum $\boldsymbol{K}$ of the pair [Eq. (43)].

An appealing scenario is realized at high transverse magnetic fields B in the strong-pairing limit, wherein the lowest-energy $S_z = +1$ channel comes into resonance with the tightly bound state of $S_z = 0$. Our model predicts formation of p-wave quantum halos and a topological BCS-BEC phase transition as B is tuned across the critical value B_c defined by Eq. (65). The obtained linear dependence of B_c on the binding energy is in agreement with the previous numerical studies [11].

Formally, our main result is demonstration of the mapping of the problem in the strong-pairing regime onto the Fano-Anderson model (77) for which the well-established solutions are known. The many-body physics then proves to be almost identical to that of resonantly paired p-wave Fermi superfluids [31]. A difference is the synthetic origin of the angular momentum in our case. Emergence of the angular momentum for Cooper pairs may be interpreted similarly to the formation of quantum halo in vacuum: the bare s-wave bound state becomes dressed by the polarized Fermi sea due to the SO coupling. Conversely, the SO coupling to the bound state produces an effective p-wave attraction for the lower-energy polarized continuum. Such "pseudorotation" of the condensate disappears on the BEC side of the topological transition, where one is left with the BEC of the bare s-wave molecules.

It would be interesting to see if the quantum fluctuations may result in abrupt jump of the synthetic angular momentum (i.e., render the transition first order).

Another noteworthy direction for future research is to superimpose the SO-induced resonant coupling with a natural s-wave resonance in the bare potential (the regime with $\varepsilon > 0$ and finite width Γ, see Sec. II). Such model may apply to ultracold atomic mixtures with the usual Feshbach-resonant interactions and artificially created SO coupling. Particular interest represents the case $\varepsilon \gg 2\mu \gg \mu_B \mathrm{g} B$. In the limit of vanishing natural width of the resonance $\Gamma \to 0$, an instability of the Fermi sea would be uniquely due to the SO coupling. In contrast to the two-channel model given by Eq. (77), here both spin components would experience weak synthetic p-wave attraction. At zero magnetic field $B = 0$ the resulting state would be analogous to the hypothetic planar phase of the superfluid He^3 in thin films [42]. The phenomenology at finite B and Γ would follow closely that of polarized resonantly paired Fermi mixtures [43], except that the inter-component s-wave pairing would be supplemented with the synthetic p-wave pairings in each spin component. In contrast to He^3, the relative strengths of attraction in different channels here could be tuned by varying ε and the magnitude of the SO coupling υ_R. We now turn again to our result (43) to notice that the synthetic p-wave pairing would not be affected by the finite c.m. momenta $\boldsymbol{K}$ of the pair. As such, one may speculate on possible existence of a Fulde-Ferrel-Larkin-Ovchinnikov (FFLO) phase [44,45] with nontrivial topological properties. We note that the already existing proposals of topological FFLO superfluidity under SO coupling rely on the pairing within a single branch and require an in-plane magnetic field [46], so that further investigations along the lines suggested here could potentially add a new dimension to this interesting topic.

We have also implicitly encountered the folded-resonance scenario in our recent study of bosonic pairing [26]. The SO-coupled depairing of a bosonic molecule was shown to be greatly enhanced at the s-wave unitarity, to the extent that the pair-breaking excitation spectrum developed a roton-like minimum signaling a transition to a striped phase. The affinity of this phase to the spontaneous exciton supercurrent at the biexciton Mott transition in high magnetic fields was also discussed [47]. The consideration of fermionic pairing presented here complements those studies and enlarges the scope of the subject.

[1] L. P. Gor'kov and E. I. Rashba, Phys. Rev. Lett. **87**, 037004 (2001).

[2] A. V. Chaplik and L. I. Magarill, Phys. Rev. Lett. **96**, 126402 (2006).

[3] L. Fu and C. L. Kane, Phys. Rev. Lett. **100**, 096407 (2008).

[4] C. Zhang, S. Tewari, R. M. Lutchyn, and S. Das Sarma, Phys. Rev. Lett. **101**, 160401 (2008).

[5] J. D. Sau, R. M. Lutchyn, S. Tewari, and S. Das Sarma, Phys. Rev. Lett. **104**, 040502 (2010).

[6] J. Alicea, Phys. Rev. B **81**, 125318 (2010).

[7] M. Sato, Phys. Rev. B **79**, 214526 (2009).

[8] Y. Tanaka, T. Yokoyama, A. V. Balatsky, and N. Nagaosa, Phys. Rev. B **79**, 060505(R) (2009).

[9] S. Takei, C.-H. Lin, B. M. Anderson, and V. Galitski, Phys. Rev. A **85**, 023626 (2012).

[10] L. He and X.-G. Huang, Phys. Rev. Lett. **108**, 145302 (2012).

[11] K. Thompson, J. Brand, and U. Zülicke, Phys. Rev. A **101**, 013613 (2020).

[12] E. I. Rashba, Sov. Phys.–Solid State **2**, 1109 (1960) [Fizika tverd. tela **2**, 1224 (1960)].

[13] F. T. Vas'ko, Pis'ma Zh. Eksp. Teor. Fiz. **30**, 574 (1979) [Sov. Phys. JETP Lett. **30**, 541 (1979)].

[14] Y. A. Bychkov and E. I. Rashba, Pis'ma Zh. Eksp. Teor. Fiz. **39**, 66 (1984) [Sov. Phys. JETP Lett. **39**, 78 (1984)].

[15] G. Dresselhaus, Phys. Rev. **100**, 580 (1955).

[16] M. I. Dyakonov and V. Y. Kachorovskii, Sov. Phys.–Semicond. **20**, 110 (1986).

[17] N. Read and D. Green, Phys. Rev. B **61**, 10267 (2000).

[18] D. A. Ivanov, Phys. Rev. Lett. **86**, 268 (2001).

[19] A. J. Leggett, in *Modern Trends in the Theory of Condensed Matter*, edited by A. Pękalski and J. A. Przystawa (Springer, Berlin, 1980), pp. 13–27.

[20] G. C. Strinati, P. Pieri, G. Röpke, P. Schuck, and M. Urban, Phys. Rep. **738**, 1 (2018).

[21] E. Timmermans, P. Tommasini, M. Hussein, and A. Kerman, Phys. Rep. **315**, 199 (1999).

[22] H. Zhai, Rep. Prog. Phys. **78**, 026001 (2015).

[23] L. Huang, Z. Meng, P. Wang, P. Peng, S.-L. Zhang, L. Chen, D. Li, Q. Zhou, and J. Zhang, Nat. Phys. **12**, 540 (2016).

[24] Z. Fu, L. Huang, Z. Meng, P. Wang, L. Zhang, S. Zhang, H. Zhai, P. Zhang, and J. Zhang, Nat. Phys. **10**, 110 (2014).

[25] M. Randeria, J.-M. Duan, and L.-Y. Shieh, Phys. Rev. Lett. **62**, 981 (1989).

[26] S. V. Andreev, Phys. Rev. B **103**, 184503 (2021).

[27] U. Fano, Phys. Rev. **124**, 1866 (1961).

[28] P. W. Anderson, Phys. Rev. **124**, 41 (1961).

[29] M. Randeria, J.-M. Duan, and L.-Y. Shieh, Phys. Rev. B **41**, 327 (1990).

[30] N. Harrison and M. K. Chan, Phys. Rev. Lett. **129**, 017001 (2022).

[31] V. Gurarie and L. Radzihovsky, Ann. Phys. **322**, 2 (2007), January Special Issue 2007.

[32] J. R. Taylor, *Scattering Theory* (Dover, Mineola, New York, 2006).

[33] J. R. Schrieffer, *Theory of Superconductivity* (Avalon, New York, 1999).

[34] M. Abramowitz and I. A. Stegun, *Handbook of Mathematical Functions with Formulas, Graphs, and Mathematical Tables* (Dover, New York, 1965).

[35] A. S. Jensen, K. Riisager, D. V. Fedorov, and E. Garrido, Rev. Mod. Phys. **76**, 215 (2004).

[36] K. Gotlieb, C.-Y. Lin, M. Serbyn, W. Zhang, C. L. Smallwood, C. Jozwiak, H. Eisaki, Z. Hussain, A. Vishwanath, and A. Lanzara, Science **362**, 1271 (2018).

[37] G. E. Volovik, Zh. Eksp. Teor. Fiz. **94**, 123 (1988) [Sov. Phys. JETP **67**, 1804 (1988)].

[38] W. Yi and G.-C. Guo, Phys. Rev. A **84**, 031608(R) (2011).

[39] J. P. Gaebler, J. T. Stewart, J. L. Bohn, and D. S. Jin, Phys. Rev. Lett. **98**, 200403 (2007).

[40] L. W. Cheuk, A. T. Sommer, Z. Hadzibabic, T. Yefsah, W. S. Bakr, and M. W. Zwierlein, Phys. Rev. Lett. **109**, 095302 (2012).

[41] M. Holten, L. Bayha, K. Subramanian, S. Brandstetter, C. Heintze, P. Lunt, P. M. Preiss, and S. Jochim, Nature (London) **606**, 287 (2022).

[42] D. R. T. Jones, A. Love, and M. A. Moore, J. Phys. C: Solid State Phys. **9**, 743 (1976).

[43] D. E. Sheehy and L. Radzihovsky, Ann. Phys. **322**, 1790 (2007).

[44] P. Fulde and R. A. Ferrell, Phys. Rev. **135**, A550 (1964).

[45] A. I. Larkin and Y. N. Ovchinnikov, Sov. Phys. JETP **20**, 762 (1965).

[46] W. Zhang and W. Yi, Nat. Commun. **4**, 2711 (2013).

[47] S. V. Andreev, Phys. Rev. B **106**, 155157 (2022).